Near-field phase correction for superresolution enhancement

Kwangchil Lee, Youngjean Jung, and Kyoungsik Kim*
School of Mechanical Engineering, Yonsei University, 262 Seongsanno, Seodaemun-gu, Seoul 120-749, Korea
(Received 29 June 2009; published 30 July 2009)

Although superresolution can be successfully obtained by negative index materials, the unavoidable losses ultimately limits image resolution. Using the near-field active phase-correction method, we theoretically predict the significant enhancement of both superresolution and transmission in a realistic lossy superlens system. In a SiC superlens system, resolvable separation between two slits significantly improves from $\lambda/4.2$ to $\lambda/14.2$ and the transmission increases 30.5 times compared to the conventional index match method.

DOI: 10.1103/PhysRevB.80.033109 PACS number(s): 42.30.Wb, 42.30.Rx, 78.20.Ci

Since the first proposal to use a subwavelength aperture to obtain a resolution beyond the diffraction limit,[1] the newly discovered near-field phenomena of electromagnetic waves have provided scientific inspirations and possibilities in various applications.[2,3] A recent notable approach to overcome the diffraction limit was the application of negative index materials (NIMs).[4,5] The NIMs develop evanescent waves to achieve resolution beyond the diffraction limit and they have been experimentally demonstrated in microwave, THz, infrared, and optical ranges.[6–13] However, a major barrier to their practical application to a realistic imaging system is the image quality deterioration due to the absorption loss in the materials. The absorption loss in the NIMs obstructs ideal image reconstruction, thus ultimately creating a limit to the resolution of the imaging system. Because of the reduced transmission in realistic systems, research on the NIMs has been focused on the improvement of transmission.[14,15]

Near-field subwavelength focusing has been recently achieved by spatially shifting and controlling the transmission and the phase of incident beam.[16,17] A field synthesis method is used to combine the spatially shifted beams after both the transmission and the phase changes using a near-field plate or transmission screen. This implies that the phase change due to absorption loss is not negligible in image quality and resolution. Since it has also been shown that the phase control in an Ag near-field superlens (NFSL) improved the visibility of a subwavelength image, near-field phase correction has been demonstrated to be an important technology for image resolution enhancement.[18,19] This phase is also important for far-field adaptive optics technology, which is widely used to ameliorate image resolution using phase retrieval feedback, as shown in Fig. 1(a). Far-field adaptive optics controls the wave front of incident light via phase retrieval feedback based on the image field measurement to compensate for aberration-induced image distortion.[20] However, it is difficult to adopt the near-field phase retrieval feedback for better image quality because the optical phase measurement is practically challenging in the near field.

In this work, we propose a near-field active phase-correction method via the index mismatch approach in order to overcome the limitations of ideal image reconstruction due to absorption loss. In this method the aforementioned phase retrieval feedback used for far field is similarly applicable to near field. It should be noted that the active phase correction can significantly enhance resolution and visibility where the loss is critical to both NFSL and the host materials of an imaging system, i.e., in the mid-infrared (mid-IR) region. Taubner *et al.*[11] demonstrated a slab mid-IR NFSL in which the SiC slab is sandwiched between two layers of SiO_2 host materials because phonon resonance frequency allows negative permittivity in the mid-IR region in polar crystal.[12] At the high-spatial-frequency limit, we used an analytic method to derive the zero phase change condition depending on the absorption of SiC NFSL and host material. Also, we applied the full-wave numerical method to investigate the resolution improvement of SiC NFSL using near-field phase correction for the realistic imaging system of finite spatial frequency.[21] The resolvable separation (separation resolution) is significantly enhanced from $\lambda/4.2$ to $\lambda/14.2$ for the visibility (V) of 0.5 and the transmission also increases 30.5 times at $k_x/k_0=10$ compared to the conventional index match method where the real part (ϵ_M') of the permittivity of NFSL has been preferably index matched to that of the host material. When the permittivities of a system are real valued, the transmission reaches the maximum in an index match case because of no reflections on the interfaces. On the other hand, in a lossy system with a nonzero imaginary part of the permittivity, the transmission does not necessarily reach the maximum in an index match case. Therefore, the transmission significantly increases in the phase-correction condition obtained in our procedure.

While the field synthesis controls transmission and phase by a fabricated spatial slot array to achieve subwavelength focusing, our method actively controls for the uniform phase for the overall large area of the slab layer by tuning the incident light's wavelength to enhance visibility, resolution,

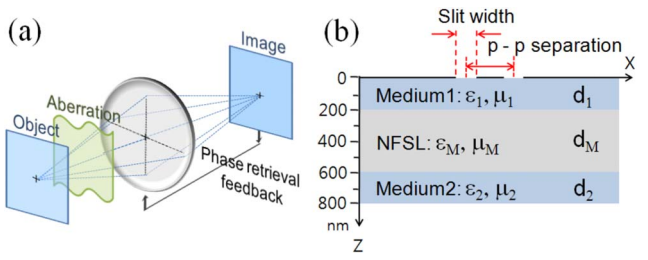

FIG. 1. (Color online) (a) In far field, adaptive optics technology is applied for image resolution improvement by phase retrieval. (b) The NFSL used in this work has schematic geometry and a double slit with a specified peak-to-peak separation and slit width; d_1 =200 nm (SiO_2), d_M=400 nm (SiC), and d_2=200 nm (SiO_2).

and transmission. Because our method requires a simple slab layer instead of complicated periodic or artificial structures, it is much easier to materialize in realistic systems. Also, the slab uniform configuration of the device facilitates area enlargement for large area imaging because the phase-correction parameter is relatively insensitive to the geometrical properties of an object. In addition, uniform wavelength tuning for the large area enables active superresolution imaging because it is unnecessary to design and optimize the device structures depending on a specific object. This characteristic of the near-field active phase correction can be easily expanded to various wavelength regions such as UV, optical, mid-IR, and THz and its structure, fabrication, and optimization processes are simple and actively tunable. Therefore, this characteristic has a profound importance for photolithography, optical nanoimaging, optical data storage, and microscopy applications.[7,10,11]

The conventional optical transfer function (OTF) from an object to an image, the ratio of the image field to the object field ($H_{\mathrm{img}}/H_{\mathrm{obj}}$), is introduced to quantify the transmission and phase change in a system.[22] The OTF is a complex function,

$$\mathrm{OTF}(k_x) = \mathrm{MTF}(k_x)\exp[-i\mathrm{PTF}(k_x)], \tag{1}$$

of which the magnitude and the phase are the modulation transfer function (MTF) and the phase transfer function (PTF), respectively.[23] The phase of the image field retrieves that of the object field if PTF=0, where the blurred image due to absorption loss can be compensated for by adopting an active phase control method.[19] The phase of OTF is actively controlled if the real part (ϵ_M') of NFSL permittivity is changed by the index mismatch case as well as the index match case through tuning the wavelength of incident light for imaging. Hence, the index mismatch approach allows us to retrieve the phase (PTF=0) of a lossy system. The transmission of the system is also evaluated by taking the square of the MTF.

Figure 1(b) shows the schematic geometry of the slab mid-IR NFSL imaging systems investigated in this work.[12] p-polarized light is incident on the 400-nm-thick SiC NFSL sandwiched between two layers of 200-nm-thick SiO_2 through a double slit with a given geometry of peak-to-peak (p-p) separation and slit width. In the symmetric case ($\epsilon_1=\epsilon_2, \mu_1=\mu_2$), the OTF is given as the multiplication of the transmission coefficient (T_p) of the slab NFSL and the wave propagation factors through the host materials as follows:[22]

$$\begin{aligned}\mathrm{OTF}(k_x) &= \exp(ik_z^{(1)}d_1)T_p(k_x)\exp(ik_z^{(2)}d_2) \\ &= \frac{t_{1M}t_{M2}\exp(ik_z^{(1)}d_1)\exp(ik_z^{(2)}d_2)}{\exp(-ik_z^{(M)}d_M)+r_{1M}r_{M2}\exp(ik_z^{(M)}d_M)},\end{aligned} \tag{2}$$

where k_x is the transverse wave vector, $k_0(=2\pi/\lambda_0)$ is the wave number of incident light, and $k_z^{(i)}$ is the z-direction wave number in i medium, $k_z^{(i)}=\sqrt{\epsilon_i\mu_i(\omega/c)^2-k_x^2}$ for $i=1,2,M$. r_{ij} and $t_{ij}(=1+r_{ij})$ are the Fresnel reflection and transmission coefficients from i medium to j medium.

At the high-spatial-frequency limit of $\omega \ll c_0\sqrt{k_x^2}$, an analytic condition for active phase retrieval can be derived for the permeabilities of all media which are identical ($\mu_M=\mu_1=\mu_2=1$). The wave numbers in the z direction inside medium $1,2,M$ are approximated as $k_z^{(1)}\simeq k_z^{(2)}\simeq k_z^{(M)}\simeq ik_x$ and r_{1M}, r_{M2} yield to

$$r_{1M} = \frac{k_z^{(1)}/\epsilon_1 - k_z^{(M)}/\epsilon_M}{k_z^{(1)}/\epsilon_1 + k_z^{(M)}/\epsilon_M} \approx -\frac{\epsilon_1-\epsilon_M}{\epsilon_1+\epsilon_M} = -r_{M2}. \tag{3}$$

As the permittivities of NFSL and the host material with absorption loss are generally represented by complex numbers ($\epsilon_M=\epsilon_M'+i\epsilon_M'', \epsilon_1=\epsilon_2=\epsilon_1'+i\epsilon_1''$), recalling $d_M=d_1+d_2$ leads the OTF in this limit ($k_x \gg k_0$) to become

$$\mathrm{OTF}(k_x) \approx \frac{1-r_{1M}^2}{\exp(2k_xd_M)-r_{1M}^2}, \tag{4}$$

where r_{1M}^2 is

$$r_{1M}^2 \approx \left[\frac{(\epsilon_1'^2-\epsilon_M'^2+\epsilon_1''^2-\epsilon_M''^2)+2i(\epsilon_1''\epsilon_M'-\epsilon_1'\epsilon_M'')}{(\epsilon_1'+\epsilon_M')^2+(\epsilon_1''+\epsilon_M'')^2}\right]^2. \tag{5}$$

To bring about phase retrieval for the NFSL imaging system, the OTF must be a real number (i.e., PTF=0) for an arbitrary $k_x(\gg k_0)$. Hence, r_{1M}^2 is supposed to be real number, which leads to the solutions of

$$\epsilon_1''\epsilon_M' - \epsilon_1'\epsilon_M'' = 0 \quad \text{or} \quad \epsilon_1'^2+\epsilon_1''^2-\epsilon_M'^2-\epsilon_M''^2 = 0. \tag{6}$$

Due to the general constraints of NFSL systems using negative dielectric lens and positive dielectric host materials ($\epsilon_M'<0, \epsilon_1'>0, \epsilon_1'', \epsilon_M''\geq 0$), the first solution of Eq. (6) requires the condition, $\epsilon_1''=\epsilon_M''=0$. This derivation implies that, in a lossless NFSL imaging system ($\epsilon_1''=\epsilon_M''=0$), the PTF is always zero and the higher transmission becomes the only compelling issue. Because there is no reflection loss on the interfaces between media, the maximum MTF is usually obtained for an impedance match case in a lossless system.[5,24] If $\epsilon_M\simeq-\epsilon_1$, then $\mathrm{OTF}\approx -4\epsilon_1\epsilon_M/(\epsilon_1-\epsilon_M)^2\simeq 1$, indicating that this medium behaves in fact as a perfect lens. Using the definition of impedance in i medium, $Z_i=\sqrt{\mu_i/\epsilon_i}$, the second solution of Eq. (6) can be rewritten as

$$|Z_1^2| = |Z_M^2|. \tag{7}$$

Besides an impedance match case, Eq. (7) extends the phase retrieval condition to an index (the real part of permittivity, ϵ') mismatch case when the absorption losses of host materials and NFSL are not negligible. In the NFSL systems with intrinsic absorptions ($\epsilon_1'', \epsilon_M''>0$), the MTF is not always the maximum in the index match case because the permittivities have nonzero imaginary parts. Therefore, phase retrieval becomes a key factor for the superlens image resolution. As the real part of NFSL permittivity is negative in this regime, ϵ_M' becomes

$$\epsilon_M' = -\sqrt{(\epsilon_1')^2+(\epsilon_1'')^2-(\epsilon_M'')^2}. \tag{8}$$

To extend the phase retrieval condition to the finite range of k_x/k_0, the full-wave numerical approach is adopted to calculate T_p and OTF. For the NFSL with finite absorption loss, the phase retrieval of OTF is achieved when the indices are mismatched.[18,19] To evaluate the improved image quality of NFSL after active phase control, we calculated the transmission field passing through a double slit aligned with the x

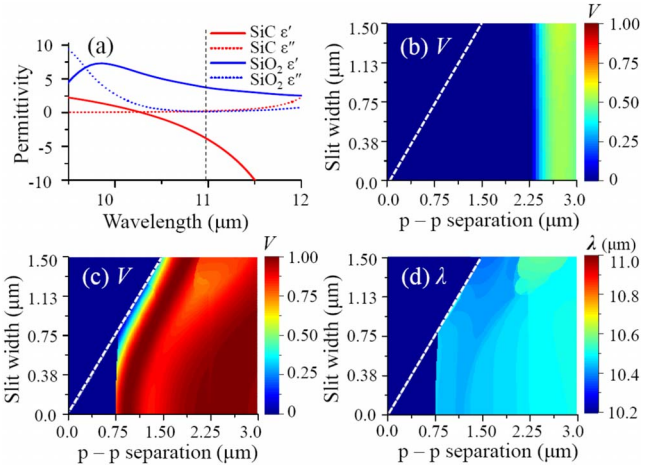

FIG. 2. (Color online) (a) The permittivities of SiC and SiO_2 depend on their wavelength. The visibilities (V) of transmission field through a double slit with given slit width and p-p separation plane are shown (b) for the index match case, (c) for the index mismatch cases with the highest visibility for each specified geometry, and (d) at the correspondingly optimized wavelength (λ) of incident light.

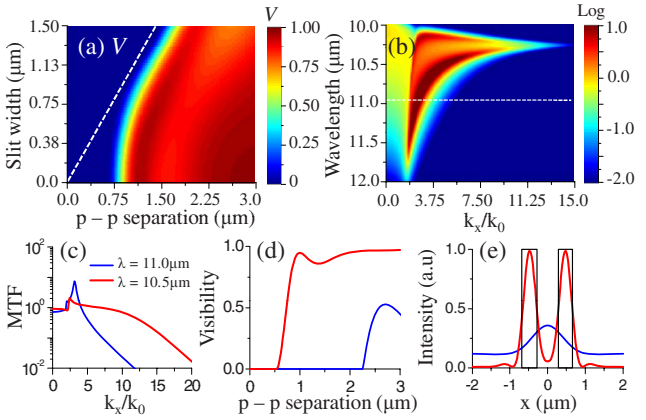

FIG. 3. (Color online) (a) The visibility in slit width and p-p separation plane when $\lambda=10.5$ μm. (b) The MTF in wavelength (λ) and k_x/k_0 plane where the white dashed line represents the index-matched wavelength. For the index-matched (11.0 μm) and phase-retrieved cases (10.5 μm), (c) the MTF as a function of k_x/k_0, (d) the visibility versus p-p separation when slit width is 360 nm, and (e) the lateral intensity distributions through a double slit with 360 nm slit width and 0.93 μm p-p separation.

axis as shown in Fig. 1(b). The field distribution at the image plane, $E_{\text{img}}(x)$, is obtained by the inverse Fourier transform of $E_{\text{obj}}(k_x)$ as follows:

$$E_{\text{img}}(x) = \frac{1}{2\pi}\int_{-\infty}^{+\infty} \text{OTF}(k_x)E_{\text{obj}}(k_x)e^{ik_x x}dk_x. \tag{9}$$

The dielectric permittivity of SiO_2 was interpolated from experimental measurements,[25] as described in Fig. 2(a), and that of SiC was derived from the dispersion relation as follows:

$$\epsilon = \epsilon' + i\epsilon'' = \epsilon_\infty \frac{\omega^2 - \omega_{LO}^2 + i\omega\Gamma_{LO}}{\omega^2 - \omega_{TO}^2 + i\omega\Gamma_{TO}}, \tag{10}$$

where $\omega_{LO}=972$ cm^{-1}, $\omega_{TO}=796$ cm^{-1}, $\epsilon_\infty=6.5$, and $\Gamma_{LO}=\Gamma_{TO}=5$ cm^{-1} including a resonance frequency of phonon mode.[12] The conventional visibility $[V\equiv(I_{max}-I_{min})/(I_{max}+I_{min})]$ of a transmission field through a double slit is used to evaluate the imaging ability of the index mismatch approach over the index match case for SiC NFSL.[26]

Figures 2(b) and 2(c) depict the visibilities parameterized by slit width and p-p separation for an index match case ($\epsilon_{\text{SiC}}=-3.71+i0.23$ and $\epsilon_{\text{SiO}_2}=3.71+i0.16$ for $\lambda=11.0$ μm) and a mismatch case with the highest visibility, respectively. Because the corresponding finite and wide range of spatial frequency is indispensable to the best visibility, we optimized ϵ_M' using the golden-section method at each specified geometry[27] and Fig. 2(d) shows the corresponding wavelength to acquire the highest visibility. With the incident light of the optimized wavelength [see Fig. 2(d)] at the specified slit width and p-p separation of the double slit, we could attain remarkably enhanced visibility [see Fig. 2(c)] throughout the region compared to that of the index match case [see Fig. 2(b)].

To form an accurate image of a complicated structure with different slit widths and separations in a realistic system, superresolution enhancement at a constant wavelength of incident light is essential. The high-performance visibility [see Fig. 3(a)] at a fixed wavelength of 10.5 μm proves that the active phase control method is useful in a practical way. Figure 3(b) depicts the MTF versus k_x/k_0 depending on wavelength. Figure 3(c) shows the MTF as a function of k_x/k_0 at the index-matched 11.0 μm and phase-retrieved 10.5 μm. In an imaging system without absorption loss, it has been widely known that the maximized MTF is usually achieved in an impedance match case because there are no reflection losses on the interfaces between media.[24] However, when the absorption loss is not negligible in the NFSL and host materials, the reflection loss needs not be minimized in the index match condition. This is clearly demonstrated in our results where the MTF in the phase-retrieved condition (the red line: $\lambda=10.5$ μm) is 30.5 times larger than that of the match case (the blue line: $\lambda=11.0$ μm) at $k_x/k_0=10$, as shown in Fig. 3(c). Figure 3(d) illustrates the visibility versus p-p separation of a double slit when the slit width is 360 nm. These results confirm that the visibility can increase significantly and a remarkable improvement of resolvable separation is achievable by using our active phase control approach. For instance, the resolvable separation for $V=0.5$ decreases from 2.6 μm (the blue line: $\lambda/4.2$ at $\lambda=11.0$ μm) to 0.74 μm (the red line: $\lambda/14.2$ at $\lambda=10.5$ μm). Figure 3(e) plots intensity of the transmitted light after the double slit of 360 nm slit width and 0.93 μm p-p separation. The intensity peaks obtained for two slits are not resolved at all (the blue line: $\lambda=11.0$ μm) in the index match case because it is beyond the diffraction limit, whereas they are well separated and resolved with higher intensity in the phase-retrieved case (the red line: $\lambda=10.5$ μm). This result suggests that 360 nm ($\lambda/29.2$)-sized object is detectable because each image intensity peak has 360 nm full width at half maximum. From these results, it is obvious that

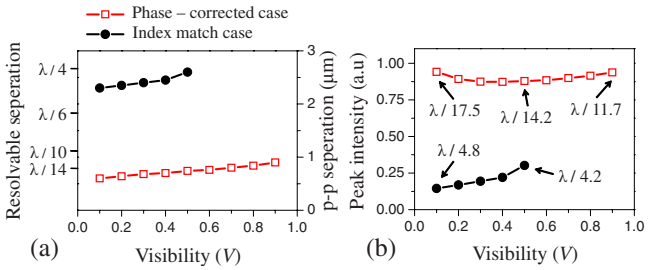

FIG. 4. (Color online) In the index match case ($\lambda=11.0\ \mu$m) and the near-field phase-corrected case ($\lambda=10.5\ \mu$m), (a) the resolvable separation (or p-p separation) between two slits with a 360 nm slit width and (b) the peak intensities of transmission are plotted depending on visibility of the image. This result predicts that we can improve separation resolution from $\lambda/4.2$ to $\lambda/14.0$ with ~ 3 times higher peak intensity for visibility=0.5.

the image resolution, visibility, and transmission can be significantly enhanced by virtue of the active phase control.

The NFSL performance improvement via the near-field phase correction is obvious if we compare the resolvable separation and transmission peak intensity for the required image visibility between the index match case (the solid circle: $\lambda=11.0\ \mu$m) and the phase-corrected case (the open square) at a fixed wavelength of $\lambda=10.5\ \mu$m. The resolvable separation (or p-p separation) between two slits of a 360 nm slit width is predicted to obtain images of various quality (visibility) in Fig. 4(a). For the visibility of $V=0.5$, for example, the resolvable separation significantly improves from $\lambda/4.2$ to $\lambda/14.2$. Also, the phase-correction method enables us to achieve a higher quality image of $V>0.6$ with resolvable separation of $\sim\lambda/12$, which is not possible even for $\sim\lambda/4$ resolution with a typical index match method. Figure 4(b) shows the transmission peak intensity through a double slit with a 360 nm slit width to get the required image visibility while minimizing the p-p separation. For $V=0.5$, along with the superior resolvable separation of $\lambda/14.2$ the transmission peak intensity becomes ~ 3 times higher than the index match case of $\lambda/4.2$. To mismatch the index for enhanced superresolution, changes in ϵ'_M of the slab NFSL can be made by tuning the wavelength of incident light into 10.5 μm for SiC [see Fig. 3(a)]. The present work is experimentally feasible with available light sources, tunable CO_2 lasers, and FTIR microscopes.[11,12]

In conclusion, the near-field active phase-correction method enables us to significantly enhance both superresolution and transmission. The resolvable separation between two slits for visibility=0.5 is ameliorated from $\lambda/4.2$ to $\lambda/14.2$ and the transmission increases by 30.5 times at $k_x/k_0=10$ for SiC NFSL compared to the typical index match method. This near-field phase-correction method can be extended to the development of a high-performance superlens from the visible to the THz region with non-negligible absorption loss.

This study was supported by grants from the National R&D Program for Cancer Control, Ministry of Health & Welfare, Republic of Korea (Grant No. 0720170), a Korea Research Foundation Grant provided by the Korean Government (MOEHRD, Basic Research Promotion Fund under Grant No. KRF-2007-331-C00121), and the National Research Foundation of Korea (NRF) funded by the Ministry of Education, Science and Technology (2009-0077097).

*Corresponding author; kks@yonsei.ac.kr

[1] E. H. Synge, Philos. Mag. **6**, 356 (1928).
[2] L. Martin-Moreno, F. J. Garcia-Vidal, H. J. Lezec, A. Degiron, and T. W. Ebbesen, Phys. Rev. Lett. **90**, 167401 (2003).
[3] T. W. Ebbesen, H. J. Lezec, H. F. Ghaemi, and T. Thio, Nature (London) **391**, 667 (1998).
[4] V. G. Veselago, Sov. Phys. Usp. **10**, 509 (1968).
[5] J. B. Pendry, Phys. Rev. Lett. **85**, 3966 (2000).
[6] D. R. Smith, W. J. Padilla, D. C. Vier, S. C. Nemat-Nasser, and S. Schultz, Phys. Rev. Lett. **84**, 4184 (2000).
[7] N. Fang, H. Lee, C. Sun, and X. Zhang, Science **308**, 534 (2005).
[8] W. Cai, D. A. Genov, and V. M. Shalaev, Phys. Rev. B **72**, 193101 (2005).
[9] H. J. Lezec, J. A. Dionne, and H. A. Atwater, Science **316**, 430 (2007).
[10] M. Alkaisi, R. J. Blaikie, and S. McNab, Adv. Mater. **13**, 877 (2001).
[11] T. Taubner, D. Korobkin, Y. Urzhumov, G. Shvets, and R. Hillenbrand, Science **313**, 1595 (2006).
[12] D. Korobkin, Y. Urzhumov, and G. Shvets, J. Opt. Soc. Am. B **23**, 468 (2006).
[13] T. J. Yen, W. J. Padilla, N. Fang, D. C. Vier, D. R. Smith, J. B. Pendry, D. N. Basov, and X. Zhang, Science **303**, 1494 (2004).
[14] J. T. Shen and P. M. Platzman, Appl. Phys. Lett. **80**, 3286 (2002).
[15] V. A. Podolskiy and E. E. Narimanov, Opt. Lett. **30**, 75 (2005).
[16] A. Grbic, L. Jiang, and R. Merlin, Science **320**, 511 (2008).
[17] L. Markley, A. M. H. Wong, Y. Wang, and G. V. Eleftheriades, Phys. Rev. Lett. **101**, 113901 (2008).
[18] K. Lee, H. Park, J. Kim, G. Kang, and K. Kim, Opt. Express **16**, 1711 (2008).
[19] K. Lee, Y. Jung, G. Kang, H. Park, and K. Kim, Appl. Phys. Lett. **94**, 101113 (2009).
[20] V. Yu. Ivanov, V. P. Sivokon, and M. A. Vorontsov, J. Opt. Soc. Am. A **9**, 1515 (1992).
[21] N. Fang and X. Zhang, Appl. Phys. Lett. **82**, 161 (2003).
[22] N. Fang, Z. Liu, T. J. Yen, and X. Zhang, Opt. Express **11**, 682 (2003).
[23] D. O. S. Melville and R. J. Blaikie, Physica B **394**, 197 (2007).
[24] A. L. Pokrovsky and A. L. Efros, Appl. Opt. **42**, 5701 (2003).
[25] E. D. Palik, *Handbook of Optical Constants of Solids* (Academic, New York, 1985).
[26] C. P. Moore, M. D. Arnold, P. J. Bones, and R. J. Blaikie, J. Opt. Soc. Am. A **25**, 911 (2008).
[27] C. He, Y. F. Zheng, and S. C. Ahalt, IEEE Trans. Multimedia **4**, 528 (2002).